IEEE Access
Multidisciplinary | Rapid Review | Open Access Journal

Received December 4, 2020, accepted December 23, 2020, date of publication December 30, 2020,
date of current version January 13, 2021.

Digital Object Identifier 10.1109/ACCESS.2020.3048022

A Novel Solar Photovoltaic Fed TransZSI-DVR for Power Quality Improvement of Grid-Connected PV Systems

ALI MOGHASSEMI[1], SANJEEVIKUMAR PADMANABAN[1], (Senior Member, IEEE), VIGNA K. RAMACHANDARAMURTHY[2], (Senior Member, IEEE), MASSIMO MITOLO[3] (Fellow, IEEE), AND MOHAMED BENBOUZID[3,4], (Fellow, IEEE)

[1]Department of Energy Technology, Aalborg University, 6700 Esbjerg, Denmark
[2]Department of Electrical Power Engineering, College of Engineering, Institute of Power Engineering, Universiti Tenaga Nasional, Selangor 43000, Malaysia
[3]School of Integrated Design, Engineering and Automation, Irvine Valley College, Irvine, CA 92618, USA
[4]Institut de Recherche Dupuy de Lôme (UMR CNRS 6027), University of Brest, 29238 Brest, France

Corresponding authors: Sanjeevikumar Padmanaban (san@et.aau.dk) and Vigna K. Ramachandaramurthy (vigna@uniten.edu.my)

The work was supported by Universiti Tenaga Nasional, Malaysia and the Long-Term Research Grant (LRGS) from the Ministry of Education Malaysia, for the program titled "Decarbonisation of Grid with an Optimal Controller and Energy Management for Energy Storage System in Microgrid Applications."

ABSTRACT In this article, a new solar PV fed Dynamic Voltage Restorer (DVR) based on Trans-Z-source Inverter (TransZSI) is proposed to improve the power quality of on-grid Photovoltaic (PV) systems. DVR is a power electronic compensator using for injecting the desired voltage to the Point of Common Coupling (PCC) as per the voltage disturbance. In the proposed DVR, in place of traditional VSI, TransZSI with outstanding merits of buck/boost, a broader range of voltage boost gain, fewer passive components, and lower voltage stress, is put forth. For efficient detection, accurate voltage disturbances mitigation, and also lessening the injected voltage harmonics, a hybrid Unit Vector Template with Maximum Constant Boost Control (UVT-MCBC) method is proposed for TransZSI-DVR. The performance of the proposed TransZSI-DVR with UVT-MCBC has been analyzed under severe sag, slight sag with harmonics, swell, and interruption. The comparative studies and simulation results have shown the effectiveness of the proposed TransZSI-DVR, as opposed to traditional ZSI-DVR and VSI-DVR. The TransZSI-DVR in the PV system has mitigated voltage sag/swell/interruption. It has also improved the power quality of both the injected voltage to the PCC and PV system's output voltage.

INDEX TERMS PV, DVR, TransZSI, voltage sag, voltage transient, THD.

NOMENCLATURE

AC	Dynamic Voltage Restorer
BES	Alternating Current
CSI	Battery Energy Storage
DC	Current Source Inverter
DVR	Direct Current
EZSI	Embedded Impedance Source Inverter
IC	Incremental Conductance
IEEE	Institute of Electrical and Electronics Engineers
IGBT	Insulated-Gate bipolar transistor
LCCT	Inductor/Capacitor/Capacitor/Transformer
MBC	Maximum Boost Control
MCBC	Maximum Constant Boost Control
MPP	Maximum Power Point
MPPT	Maximum Power Point Tracking
PCC	Point of Common Coupling
PLL	Phase-Locked loop
PV	Photovoltaic
PWM	Pulse-Width Modulation
RMS	Root Mean Square
SBC	Simple Boost Control
SLD	Single Line Diagram
SOC	State of Charge
ST	Shoot-Through
STC	Standard Test Conditions
THD	Total Harmonic Distortion

The associate editor coordinating the review of this manuscript and approving it for publication was Eklas Hossain.

TransZSI	Trans-Z-Source Inverter
TransZSI-DVR	Trans-Z-Source Inverter Based Dynamic Voltage Restorer
UVT	Unit Vector Template
UVT-MCBC	Unit Vector Template with Maximum Constant Boost Control
VSC	Voltage Source Controller
VSI	Voltage Source Inverter
VSI-DVR	Voltage Source Inverter Based Dynamic Voltage Restorer
ZSI	Impedance Source Inverter
ZSI-DVR	Impedance Source Inverter Based Dynamic Voltage Restorer

I. INTRODUCTION

For environmental concerns and development towards a sustainable society, the future power systems will have a high penetration of solar PV and wind power systems. The trend is towards ramping up renewable energies and phasing out fossil fuels and coal. Out of renewable energy sources, PV systems have been significantly tilted towards because the sunlight is one of the most abundant and freely available energy resources on our planet [1]. However, the performance of the PV systems can be handed down affected by factors like solar irradiation, temperature, soiling, clouds, etc. resulting in a reduction in the PV output voltage and therefore, voltage sag, as the most commonplace yet vital power quality issues, happens. With an increase in the number of sensitive and critical loads in the modern power system, power quality issues like sags, swells or interruptions have enlarged. Such power quality issues result in considerable losses such as losses related to producer's competitive opportunities, reduced efficiency, increased production and maintenance costs, reduced product quality, decreased equipment lifespan, and production interruptions and energy losses. Having high-quality power Thus, accessing high-quality power has a tremendous impact on saving capital and has an economic advantage for a manufacturing company [2]–[4].

High power quality produces an impeccable power supply that has no noise, sinusoidal waveform, is always available, and within voltage and frequency tolerances. Voltage sags/swells/interruptions are the most important power quality issues which are classified as short-duration voltage variations [5]. As per the standard IEEE 1159 [6], voltage sag is a fall in the Root Mean Square (RMS) voltage (0.1–0.9pu of nominal voltage) the duration of which is 0.5$cycles$-1min. The root causes of sags are usually the faults and starting of large loads like motors. In grid-connected PV systems, partial shading condition is the leading cause of voltage sags. Also, a voltage swell is a rise in the RMS voltage (1.1–1.8pu of nominal voltage) at the same duration as voltage sag. The start/stop of large capacitors and turning off the large loads are the leading causes of swells.

There are many methods to avoid the impact of such voltage disturbances on sensitive and critical loads. The most efficient and reasonable one is to apply devices that are built based on power converters, aka custom power devices [7]. Among them, Dynamic Voltage Restorer (DVR) is the most efficient device of choice for the mitigation of voltage sags, swells, and interruptions. DVR is connected in series to the PCC between the load and source sides, and in healthy conditions, the DVR is in standby mode. Once the supply voltage goes upper or lower than its nominal value, the DVR controller detects the magnitude and duration of the supply voltage and then injects the desired voltage to the PCC accordingly. A DVR is composed of a DC storage unit, a voltage source inverter (VSI), an LC filter, and three single-phase injection/coupling transformers [8].

The VSI has been traditionally employed in the DVR configuration [9]. In [10], the performance of the DVR system based on the VSI is investigated, and simulation is performed for voltage sag and voltage swell situations. The DVR system can easily handle and keep the voltage balanced and constant, which is required by the load. Although the VSI is widely used in DVR configuration, it has some limitations [11]. Being a buck converter, it needs a DC/DC boost converter. Also, in each leg, the semiconductors are not turned ON at the same time; otherwise, shoot-through (ST) happens and damage the inverter bridge. Note that the ST is brought about by simultaneously turning on both switches in the 1φ leg, 2φ legs, or all 3φ legs, thus short-circuiting the supply. Like VSI, Current Source Inverter (CSI) needs a buck converter and leastways one upper or lower semiconductor has to be turned on.

To address the limitations mentioned above, Impedance Source Inverter (ZSI) has been proposed [11]. The ZSI employs an X shape impedance circuit, including two capacitors and two inductors to not only join the primary circuit to the load side but to bring significant benefits CSI and VSI lack. In the ZSI, the value of the AC output voltage has nothing to do with the DC input voltage and can be anything between $[0, \infty]$. Thus, the ZSI is a buck and boost converter simultaneously and has a wider voltage gain range. So, in place of VSI, the great idea is to use ZSI in the DVR configuration. ZSI-DVR configuration has been studied in [12]–[21]. In [12], ZSI-DVR was presented in which a multi-loop controller was used, and the results showed that the proposed DVR used the buck/boost advantages of ZSI to employ the energy storage while compensating for sag ultimately. However, the only studied voltage disturbance in this article was sag. Also, the traditional Pulse-width Modulation (PWM) was implemented. Similar work was done in [13] in which efficient and straightforward open-loop sag/swell and closed swell controllers were studied. In [14], the analysis of ZSI-DVR with a fuzzy controller was conducted, and the simulation results showed a better performance of the proposed ZSI-DVR optimized by the fuzzy controller. To improve the ride-through capability of ZSI-DVR, wind turbine as renewable energy sources is offered in [15]. However, the wind turbine has a wind generation and a rectifier which could increase the DVR complexity and cost. Supercapacitor-based

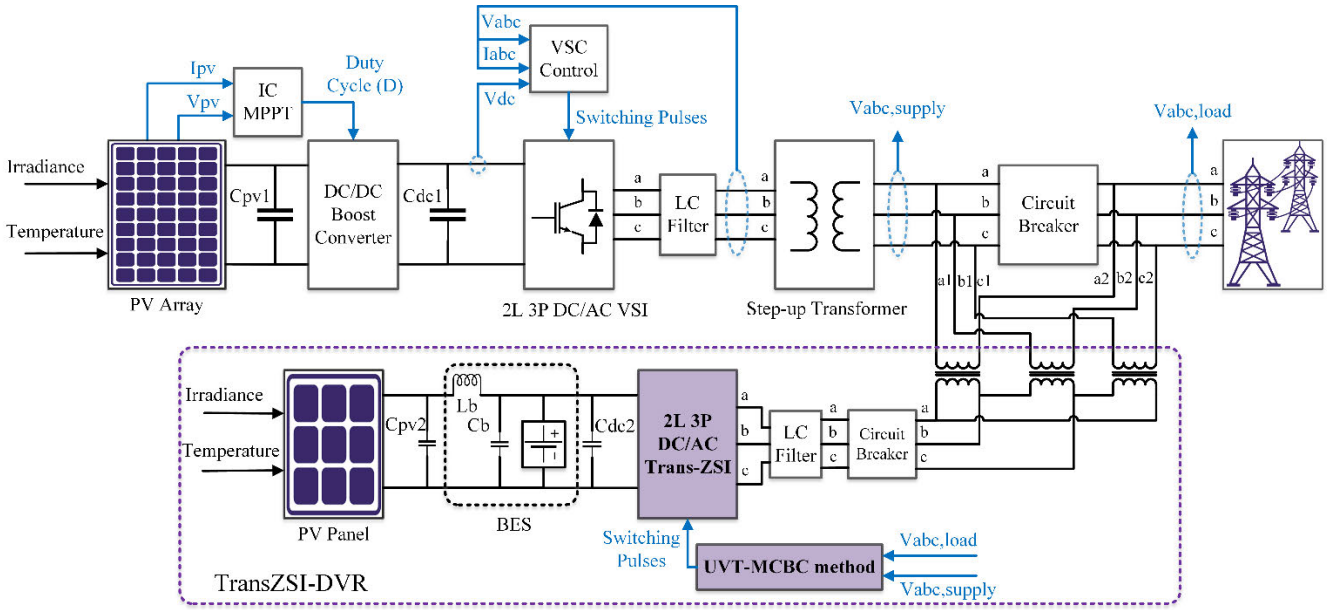

FIGURE 1. Proposed PV fed TransZSI-DVR configuration.

ZSI-DVR as its energy storage was presented in [16] to create DC voltage of ZSI. Supercapacitors can charge fast and discharge very slow.

To increase the voltage-gain and decrease the voltage stress of ZSIs, some modified configurations were proposed [17]. Recently, some studies have been carried out to enhance DVR's performance based on such modified ZSI arrangements [18]–[21]. Cascaded multilevel ZSI for DVR was proposed in [18] to decrease the voltage THD. In [19], embedded EZSI based DVR was presented to mitigate balanced/unbalanced voltage sags caused by different faults. The results proved that the proposed DVR is simple to implement, and its cost is low. New LCCT-ZSI based DVR was introduced in [20], which can provide higher voltage gain. However, THD analysis and performance evaluation for swell and interruption were neglected. YSI based DVR with Fuel Cell was studied in [21], and with the help of the fuzzy controller, the THD was reduced, as opposed to ZSI-DVR.

Among the modified ZSI configurations presented in [18], TransZSI that uses a capacitor and a transformer as its impedance network has delivered a standout performance. Compared to ZSI, by the transformer's turns ratio, a higher voltage gain is obtained in the TransZSI. Plus, the number of passive elements is reduced, thus reducing the costs and increasing the inverter's lifetime and reliability. As a result, this article tries to propose a new PV fed DVR configuration based on TransZSI in which an integration of PV panel and batteries is presented. This will help the issue related to the capture of energy in PV panels and issue related to the energy reserves of batteries. To boost the efficacy of the DVR controller and provide an accurate detection method and efficient compensation for voltage sags/swells/interruptions, a hybrid unit vector template (UVT) with an MCBC method

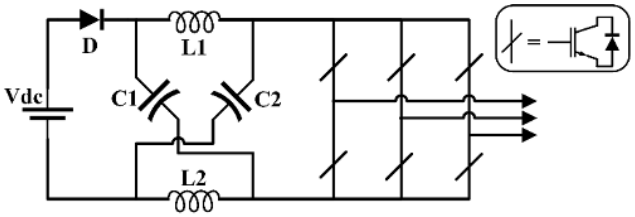

FIGURE 2. The ZSI basic circuit topology.

(UVT-MCBC) is presented. The UVT can determine the exact start/stop points of every voltage disturbance and then creating voltage load references for the modulation unit [22].

In this article, the modulation unit is based on the MCBC method as a modified version of the conventional Simple and Maximum Boost Control methods (SBC and MBC). However, the SBC and MBC methods have both limitations [23]. The SBC method has the limit of boosting the output voltage. The modulation index decreases as the ST increases, increasing voltage stress. In the MBC method, all the zero states are used as ST states thus increasing the output voltage level. Although this method minimizes the voltage stress and maximizes the voltage gain, it creates low-frequency ripples in the current. This means the lower the output frequency, the higher the passive elements. The MCBC method can overcome such limitations. In the MCBC method, the ST duty ratio remains unchanged to bring outstanding benefits of a wider voltage gain range and no low-frequency ripples. Therefore, the UVT-MCBC can accurately detect the voltage disturbances, inject the desired voltage accordingly with lower harmonics, and compensate for them efficiently. Below, the significant contributions of this work are provided:

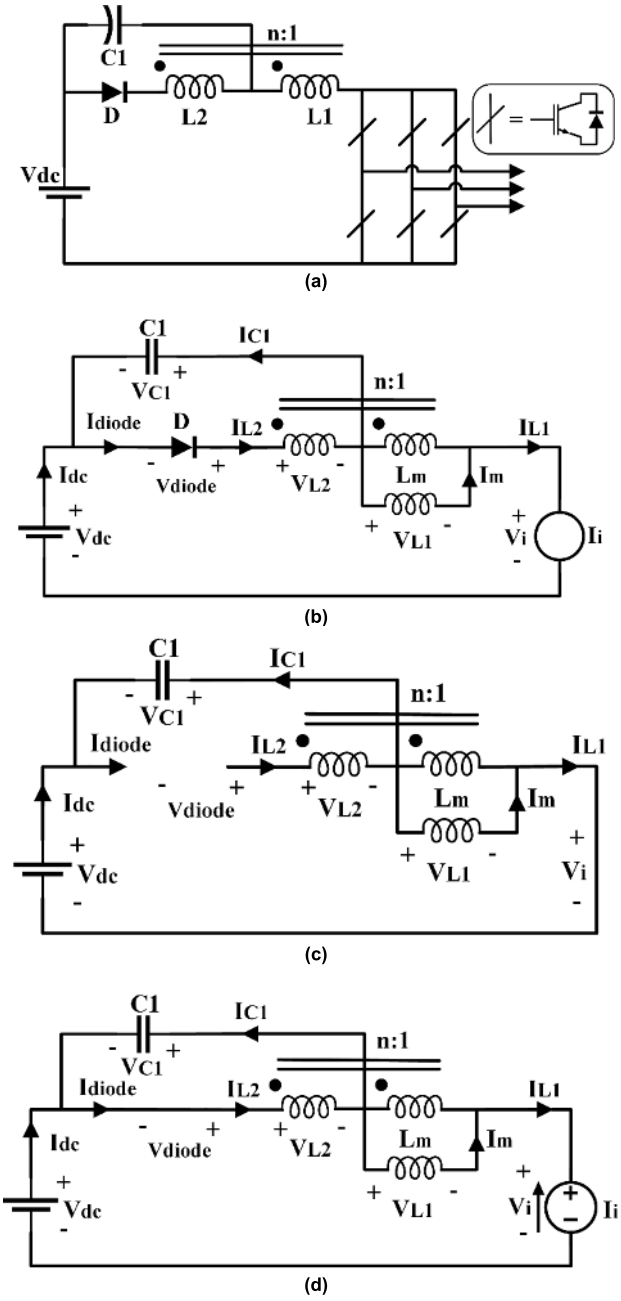

FIGURE 3. The TransZSI: (a) basic circuit, (b) with the trans., (c) in ST zero states, and (d) in non-ST states.

- A solar PV fed TransZSI-DVR is proposed in which TransZSI offers outstanding features of (1) a more comprehensive range of voltage gain, (2) lower voltage stress across the switches, and (3) fewer reactive elements.
- A UVT-MCBC is presented to improve the control performance of the TransZSI-DVR. It gives the best performance among the other two conventional DVR systems by (1) detection of start/stop points of voltage disturbances, (2) reduction in transients, (3) mitigation of voltage disturbances, and (4) reduction in injected voltage THD. So, the output PV voltage's power quality is enhanced.

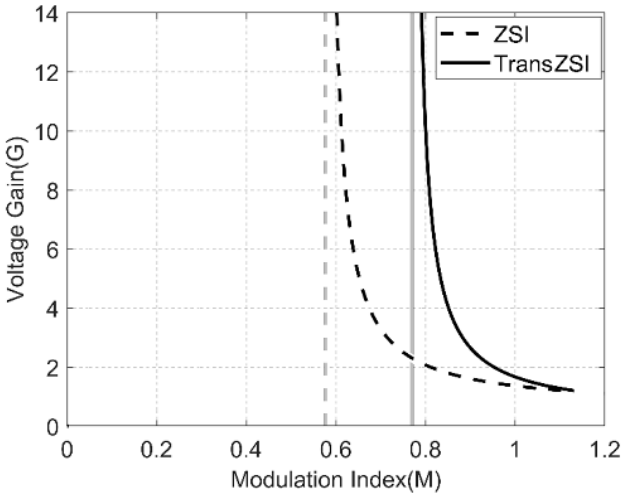

FIGURE 4. Voltage boost gain (G) against different values of M in the ZSI and TransZSI.

- Integration of the PV panel and battery is put forward for the proposed TransZSI-DVR to address the issue related to the capture of energy in PV panels and the issue related to the energy reserves of batteries. Because (1) sunlight as a freely available kind of energy lowers batteries' energy restrictions, (2) recharging batteries with solar power offers a convenient option for DVR, and (3) batteries help ease the problem related to the intermittent nature of PV panels.

The proposed solar PV fed TransZSI-DVR is described in Section 2 including the conception of TransZSI, hybrid UVT with MCBC method (UVT-MCBC), voltage stress analysis, PV array modeling, MPPT technique, boost converter, DC/AC VSI, and VSC controller. Section 3 presents the simulation outcomes and analyses, together with comparisons. And the article is concluded in Section 4.

II. PROPOSED TransZSI-DVR CONFIGURATION

Fig. 1 shows the proposed TransZSI-DVR configuration. In this figure, DVR is connected in series to the PCC on the supply side (in this article, the output of grid-connected PV system) to detect voltage disturbances including sags, swells, and interruptions and then compensate for them. The PV system comprises the PV array, MPPT controller, boost converter, DC/AC VSI, filter, 3φ transformer, and distribution network to which the PV array is connected. In normal conditions, the DVR is in standby mode. Once voltage sags, swells, and interruptions happen, the DVR detects them, and as per the amount and duration of the voltage disturbances and it then injects the desired voltage to the PCC. The DVR comprises a PV panel, Battery Energy Storage (BES), the proposed TransZSI, the proposed UVT-MCBC controller, an LC filter, and three single-phase injection transformers.

When a voltage disturbance occurs on the supply side, the energy storage in the DVR provides its desired energy. The energy storage can be a DC-link capacitor or a Battery

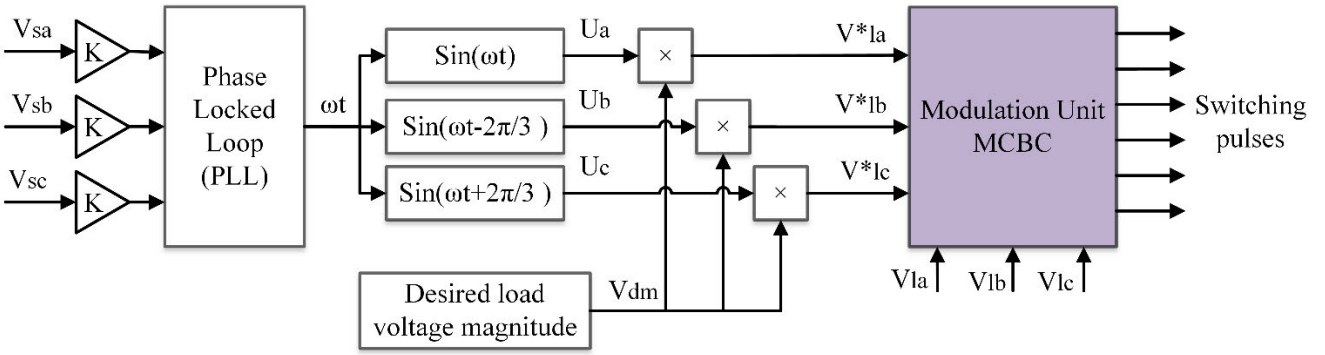

FIGURE 5. The DVR control diagram based on the UVT-MCBC method.

Energy Storage (BES). The capacitor's storage capacity is lower than the BES which is why the BES is widely used. In this article, integrating the PV panel and BES is proposed for TransZSI-DVR. On the one hand, solar energy lowers the batteries' energy restrictions. Recharging the BES with solar energy offers a convenient option for DVR. Batteries overcome the intermittency concern of PV panels. This integration serves the needs for addressing the issue related to the capture of energy in PV panels and the issue related to the energy reserves of batteries.

A. TransZSI

In this article, two traditional VSI-DVR and ZSI-DVR are considered for performance comparison with the proposed TransZSI-DVR. For VSI-DVR, UVT based on Pulse Width Modulation (UVT-PWM) is used. For both ZSI-DVR and the proposed TransZSI-DVR, the UVT-MCBC method is applied. Therefore, three different cases of VSI-DVR (UVT-PWM), ZSI-DVR (UVT-MCBC), TransZSI-DVR (UVT-MCBC) are carefully analyzed in this work. The VSI has been widely deployed to form the interface to the grid from renewable energy sources. However, VSI has limitations that have been pointed out in the literature review. ZSI, as its primary circuit is shown in Fig. 2, can address such problems [11]. In ZSI, ST is used for boosting the voltage in the VSI. So, the buck/boost feature is obtained, and the need for a boost converter is eliminated. However, traditional ZSI has some limitations. Among modified configurations of ZSI that were recently introduced to increase voltage gain and to cut down on the cost, TransZSI has shown superb performance in price, voltage gain, and voltage stress on the switches [24]. Fig. 3(a) depicts the structure of TransZSI from the DC-link viewpoint.

Similar to the ZSI, TransZSI has an additional ST zero state aside from the 6 active and 2 primary zero states. Fig. 3(b) illustrates TransZSI's equivalent circuit in which ZSI's 2 inductors are coupled and displaced by a transformer [24].

In ST zero states, the bridge is short-circuited, as shown in Fig. 3(c). Assuming D_{sh} as the ST duty ratio and T as the switching cycle, so $D_{sh}T$ and $(1 - D_{sh})\,T$ are intervals for ST and non-ST states, respectively. In ST zero states, the voltages of L_1 & L_2 are [24]:

$$v_{L1} = V_{dc} + V_{C1} \tag{1}$$

$$v_{L2} = \frac{n_2}{n_1}.v_{L1} \tag{2}$$

In non-ST zero states, the bridge is represented as a current source. The non-ST states have 6 active and 2 zero states. The current source is zero in 2 zero states. In non-ST states, as shown in Fig. 3(d), we have [24]:

$$v_{L1} = \frac{n_1}{n_2}.v_{L2} = -\frac{n_1}{n_2}.V_{C1} \tag{3}$$

$$v_{L2} = -V_{C1} \tag{4}$$

The median inductors' voltage would be 0 throughout the switching cycle (steady-state). From (1) and (3):

$$\langle v_{L1} \rangle = \frac{\left(V_{dc} + V_{C1}\right).D_{sh}.T + \left(-\frac{n_1}{n_2}.V_{C1}\right).\left(1 - D_{sh}\right).T}{T} = 0 \tag{5}$$

Based on (5), the capacitor's voltage is:

$$V_{C1} = \frac{n.D_{sh}}{1 - \left(1 + \frac{n_2}{n_1}\right).D_{sh}} V_{dc} \tag{6}$$

where $\frac{n_2}{n_1} = n \geq 1$. From (4)-(6), the DC-link voltage in the non-ST states is increased to:

$$\widehat{v_i} = \left(\frac{1}{1 - (1 + n).D_{sh}}\right) V_{dc} = B.V_{dc} \tag{7}$$

In (7), B is the boost factor:

$$B = \frac{1}{1 - (1 + n).D_{sh}} \tag{8}$$

The phase voltage's peak value viewed from the output of the inverter is:

$$\widehat{V_{ph}} = M \cdot \left(\frac{\widehat{V_i}}{2}\right) = M \cdot \left(B \cdot \frac{V_{dc}}{2}\right) \tag{9}$$

In (9), M remarks the modulation index. In turn, the voltage gain would be:

$$G = \frac{M}{1 - (1 + n).\left(1 - \frac{\sqrt{3}}{2}M\right)} \tag{10}$$

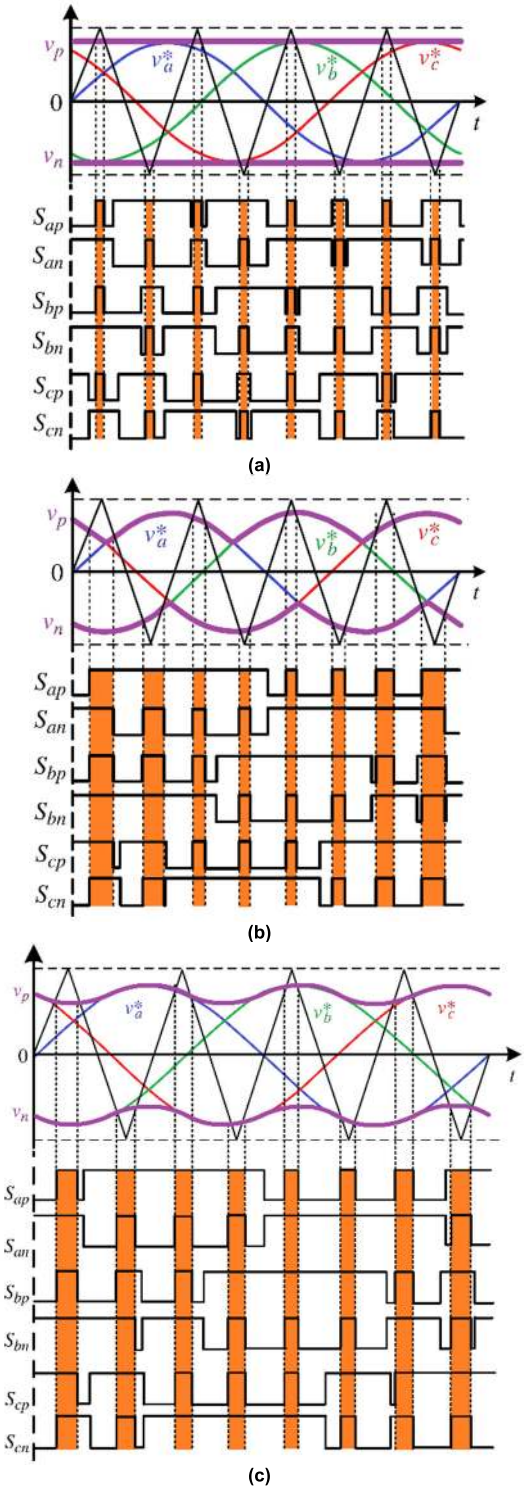

FIGURE 6. (a) SBC, (b) MBC, and (c) MCBC method schemes.

Equation (10) is calculated when the MCBC method is implemented to the TransZSI. The MCBC method will be explained in the following subsection. It is worth mentioning that when the MCBC method is used in the ZSI, the voltage gain is [23]:

$$G = \frac{M}{\sqrt{3}M - 1} \tag{11}$$

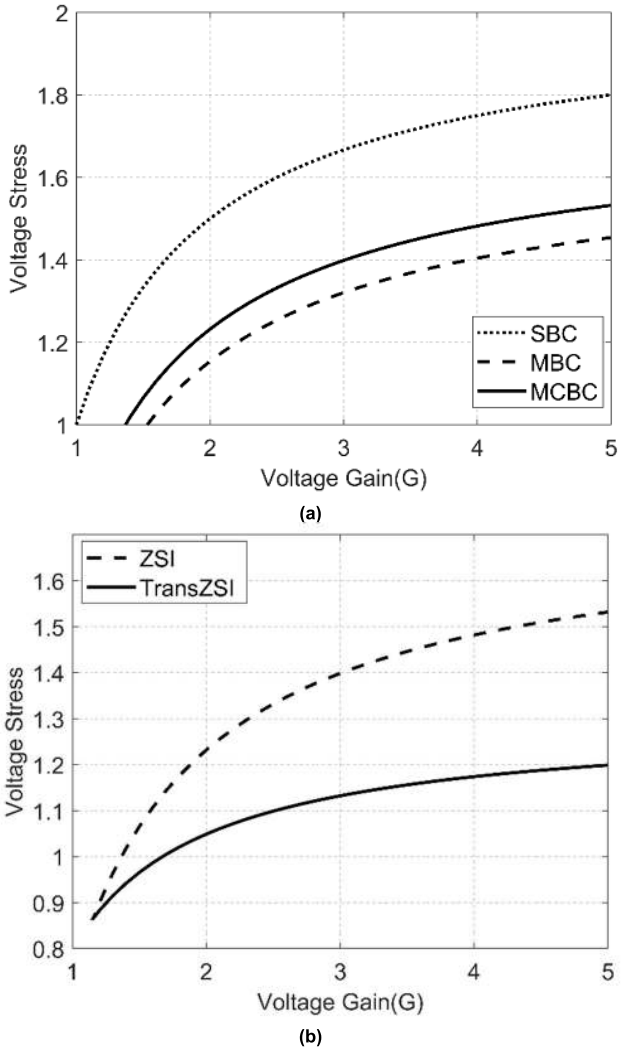

FIGURE 7. Voltage stress vs voltage gain for (a) different control methods in ZSI, (b) MCBC method in ZSI and TransZSI.

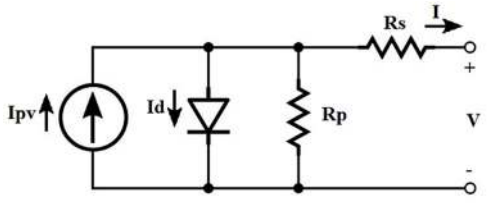

FIGURE 8. The equivalent circuit single-diode model of a PV cell.

As per (10) and (11), the voltage gain equations of ZSI and TransZSI are equal when $n = 1$. If n is higher than 1, the ZSI's voltage gain is lower than TransZSI's. So, the TransZSI's voltage gain is higher for a given modulation index (see Fig. 4). This means that in TransZSI, the ST duty ratio is lower, and the modulation index is higher.

B. TransZSI-DVR CONTROL STRATEGY

1) UNIT VECTOR TEMPLATE (UVT) METHOD

The three-phase supply voltages of V_{sa}, V_{sb}, and V_{sc} (in this article, the grid-connected PV output AC voltage) are

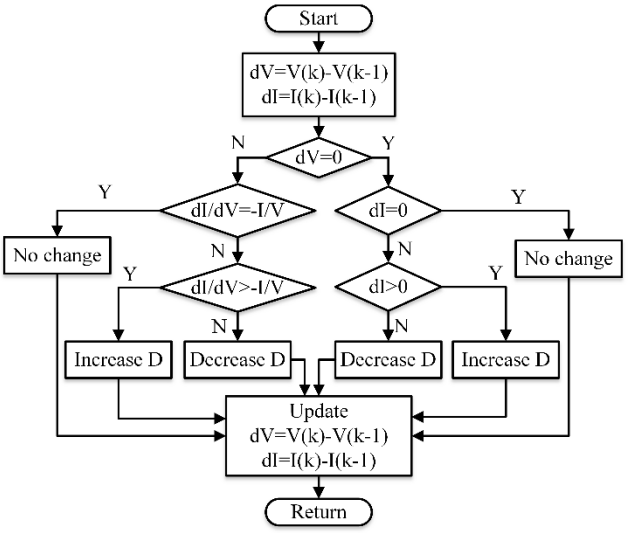

FIGURE 9. The IC algorithm's flowchart.

calculated and then multiplied by $K = 1/V_m$, where V_m is the peak magnitude of supply voltage as below [25]:

$$V_m = \sqrt{\frac{2}{3}\left(V_{sa}^2 + V_{sb}^2 + V_{sc}^2\right)} \tag{12}$$

A phase-locked loop (PLL) is applied to create sinusoidal unit vectors (U_a, U_b, U_c) by extracting transformation angle (ωt) and also to synchronize the supply voltage, as below:

$$U_a = \sin(\omega t), \quad U_b = \sin\left(\omega t - \frac{2\pi}{3}\right),$$
$$U_c = \sin\left(\omega t + \frac{2\pi}{3}\right) \tag{13}$$

Then the load reference voltages (V_{la}^*, V_{lb}^*, V_{lc}^*) are produced by comparison the sinusoidal unit vectors (U_a, U_b, U_c) to V_m, as follows:

$$\begin{aligned} V_{la}^* &= V_{dm} U_a \\ V_{lb}^* &= V_{dm} U_b \\ V_{lc}^* &= V_{dm} U_c \end{aligned} \tag{14}$$

The load reference voltages along with the measured load voltages (V_{la}, V_{lb}, V_{lc}) are given to the modulation unit to create switching pulses (S_1 to S_6) for triggering the switches of DC/AC inverter. Fig. 5 illustrates the DVR control diagram based on the UVT-MCBC method. The MCBC method will be explained in great detail in the following subsection.

2) MCBC METHOD

As discussed earlier, the higher voltage gain results in a fall in the modulation index and a rise in the voltage stress. Many PWM methods were presented to maximize voltage gain and minimize the voltage stress simultaneously [26]. The SBC method, as shown in Fig. 6(a), was presented to control ST but it is weak in maximizing the output voltage. To put it simply, the higher the ST, the lower the modulation index. Therefore, voltage stress is high. Then the MBC method, as shown in Fig. 6(b), was proposed. Although in MBC the voltage stress is significantly declined and the output voltage is boosted, it produces low-frequency ripples.

To remove such ripples, the MCBC method as illustrated in Fig. 6(c) is applied in which the ST duty ratio is kept constant [23]. By doing so, unique features like a wider range of voltage gain and lower voltage stress are obtained. This will drive down the cost and weight of the TransZSI. Based on Fig. 6(c), there are three reference curves and two ST envelope curves. The inverter is in the ST zero states once the carrier triangle wave goes over V_p or under V_n. Otherwise, the converter performs based on the basic carrier-based PWM. Based on Fig. 6(c), for each half-period we have [24]:

$$\left.\begin{aligned} V_{p_1} &= \sqrt{3}M + \sin\left(\theta - \tfrac{2\pi}{3}\right)M \\ V_{n_1} &= \sin\left(\theta - \tfrac{2\pi}{3}\right)M \end{aligned}\right\} \quad [0, \pi/3] \tag{15}$$

$$\left.\begin{aligned} V_{p_2} &= \sin(\theta)\,M \\ V_{n_2} &= \sin(\theta)\,M - \sqrt{3}M \end{aligned}\right\} \quad [\pi/3, 2\pi/3] \tag{16}$$

From (15) and (16), it can be concluded that for a specific M, the distance between V_p and V_n is always kept constant at $\sqrt{3}M$ and measures the ST. The ST duty ratio is constant:

$$D_{sh} = \frac{2 - \sqrt{3}M}{2} = 1 - \frac{\sqrt{3}M}{2} \tag{17}$$

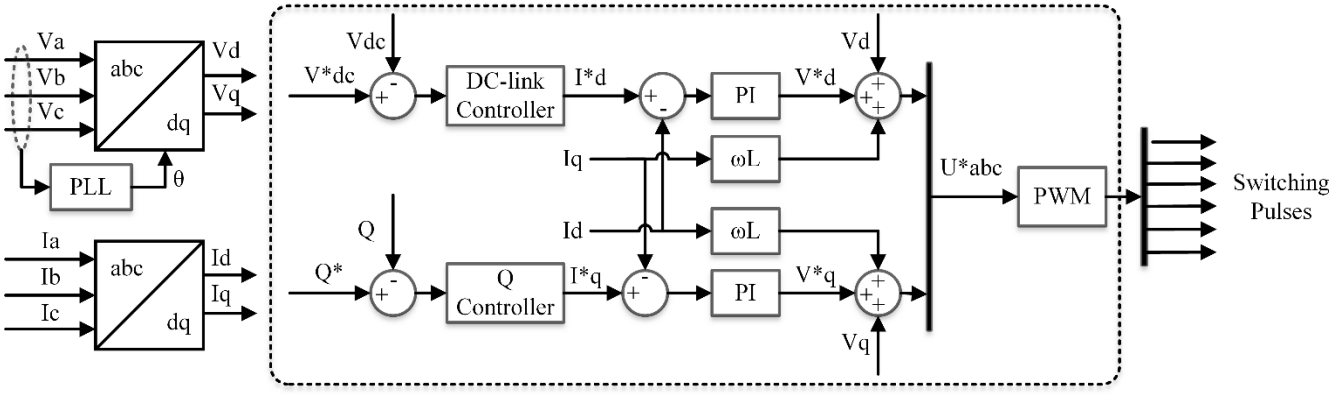

FIGURE 10. The VSC control structure.

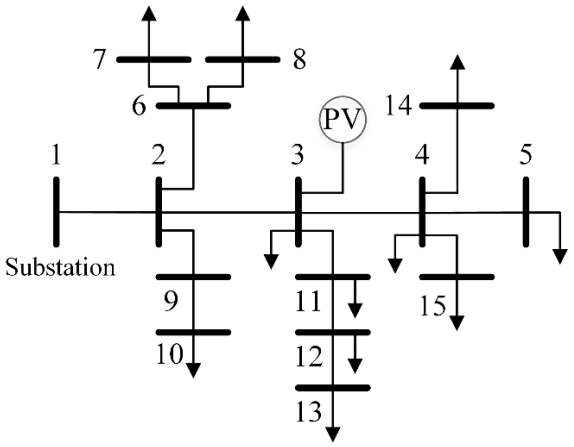

FIGURE 11. The SLD of the IEEE 15-bus grid.

3) VOLTAGE STRESS COMPARISON

The voltage stress, V_S, can be realized by comparison the minimum dc voltage (GV_{dc}) and peak dc-link [23]:

$$V_S = BV_{dc} \tag{18}$$

Fig. 7(a) provides a comparison of voltage stress in SBC, MBC, and MCBC methods applied to the ZSI. The related equations to the voltage stress ratios are [23]:

$$\frac{V_S}{GV_{dc}} = \frac{BV_{dc}}{GV_{dc}} = 2 - \frac{1}{G} \quad \text{SBC method} \tag{19}$$

$$\frac{V_S}{GV_{dc}} = \frac{BV_{dc}}{GV_{dc}} = \frac{3\sqrt{3}}{\pi} - \frac{1}{G} \quad \text{MBC method} \tag{20}$$

$$\frac{V_S}{GV_{dc}} = \frac{BV_{dc}}{GV_{dc}} = \sqrt{3} - \frac{1}{G} \quad \text{MCBC method} \tag{21}$$

By using the MCBC method in the TransZSI, we have:

$$\frac{V_S}{GV_{dc}} = \frac{BV_{dc}}{GV_{dc}} = \frac{\sqrt{3}}{2}\left(1 + \frac{1}{n}\right) - \frac{1}{nG} \tag{22}$$

Similar to the voltage gain equations of ZSI and TransZSI, if $n = 1$, the voltage stress ratio of ZSI, (21), and of TransZSI, (22) are equal. If n is higher than 1, the voltage stress ratio of TransZSI lesser than that of ZSI [24]. A comparison of voltage stress ratios of ZSI and TransZSI (when MCBC is applied) to both is provided in Fig. 7(b).

C. PV ARRAY MODELING AND MPPT ALGORITHM

A PV array comprises some PV modules that are formed by some PV cells. Fig. 8 shows an equivalent single-diode model of a PV cell [2]. In this model, I_{PV} is PV current based on solar irradiation, R_p and R_s are parallel and series branch resistors, I_D is diode current, and V and I are output voltage and current, respectively. Equation (25) describes the PV cell output current at Standard Test Conditions (STC) (radiation of $1000W/m^2$ and cell temperature of $25°C$).

$$I = I_{PV} - I_{sat}\left[\exp\left(\frac{Q \cdot V_{oc}}{A \cdot K \cdot T}\right) - 1\right] - \left(\frac{V + I \cdot R_s}{R_p}\right) \tag{23}$$

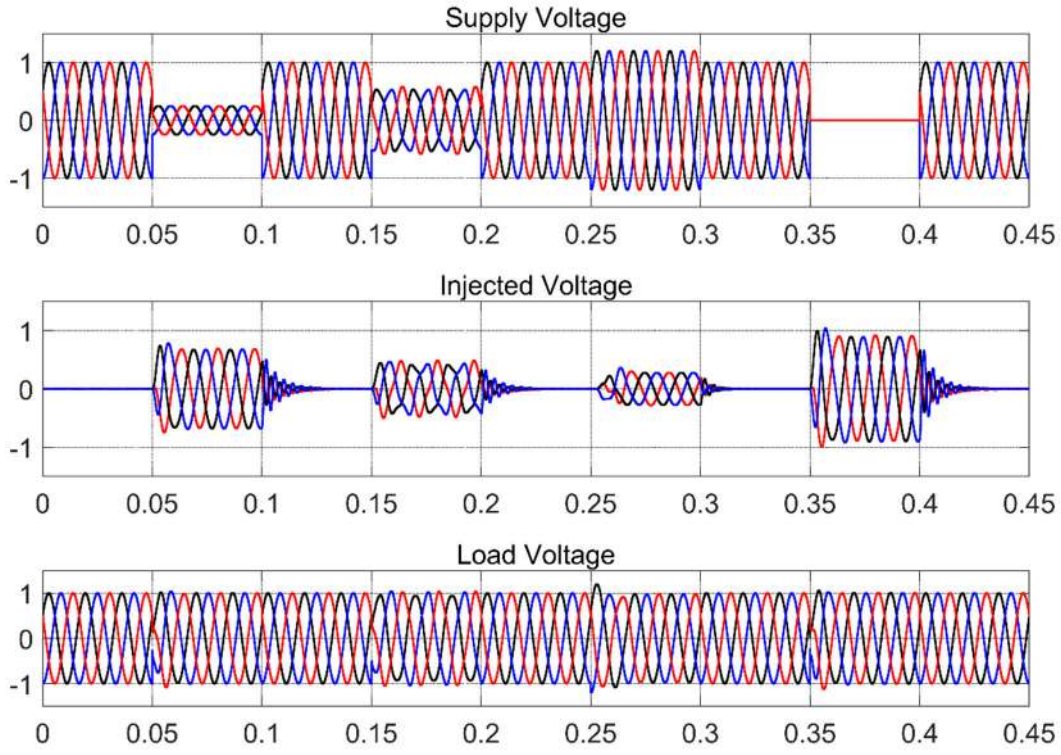

FIGURE 12. Supply, injected, and load voltage waveforms (upper, middle, and lower, respectively) in the PV fed VSI-DVR.

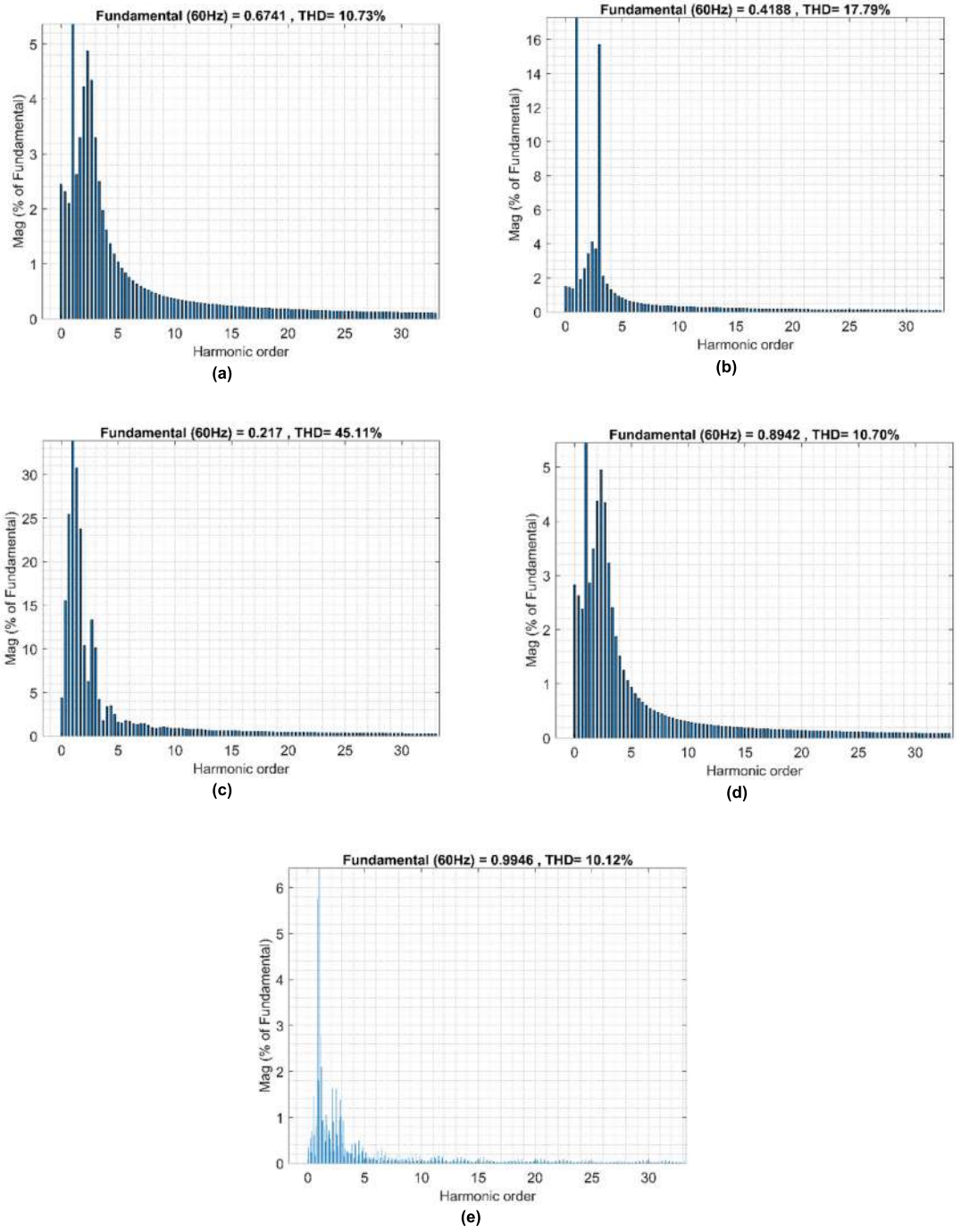

FIGURE 13. Phase A THD values of the (a) injected voltage in 0.05-0.1s, (b) injected voltage in 0.15-0.2s, (c) injected voltage in 0.25-0.3s, (d) injected voltage in 0.35-0.4s, and (e) entire load voltage in 0-0.45s.

where I_{sat} is the diode saturation current, Q is the electron charge, A is the diode propagation coefficient, K is the Boltzmann constant, and T is the cell's real temperature. PV systems are highly affected by solar irradiation and temperature. Obtaining maximum PV power is of importance, to this end, an accurate MPPT technique can find the maximum power point (MPP) of the PV system [27]. In this work, we used the Incremental Conductance (IC) technique which is on the basis of the measurement of the output PV voltage by comparing instantaneous and incremental conductance. If these two values are equal, the MPP is reached. An IC MPPT controller optimizes the switching duty cycle (D) to create the desired voltage, obtaining the MPP. Fig. 9 shows the IC algorithm's flowchart.

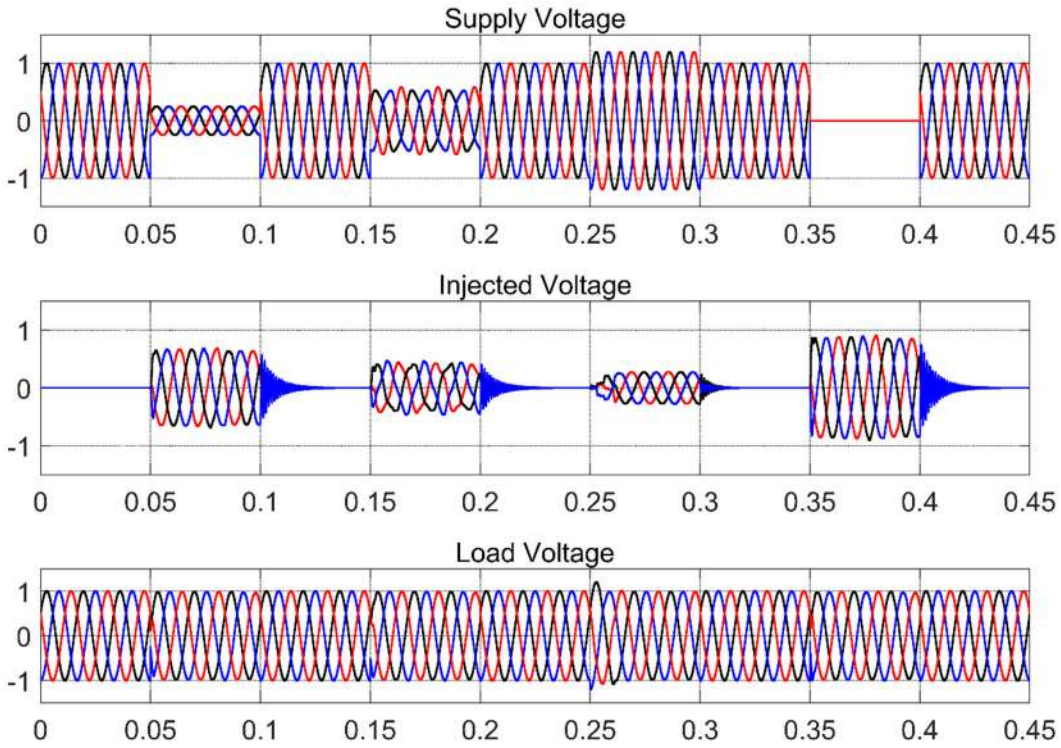

FIGURE 14. Supply, injected, and load voltage waveforms (upper, middle, and lower, respectively) in the PV fed ZSI-DVR.

TABLE 1. Comparison of Voltage THD Measured in Different DVR Scenarios.

Scenario		Injected Voltage THD (%)				Load Voltage THD (%)	
	Phase	0.05-0.1s Severe Sag	0.15-0.2s Slight Sag	0.3-0.35s Swell	0.4-0.45s Interruption	0-0.45s Total	Reduction
VSI-DVR	φa	10.73	17.79	45.11	10.70	10.12	-
	φb	19.93	24.75	27.58	18.39	11.43	-
	φc	23.16	27.23	28.59	21.85	10.26	-
ZSI-DVR	φa	3.39	13.10	40.14	3.29	8.51	15.90
	φb	10.19	16.15	29.43	8.51	8.79	23.09
	φc	12.42	17.82	29.27	10.22	8.20	20.07
Proposed TransZSI-DVR	φa	2.42	10.90	38.22	2.09	**5.14**	**49.20**
	φb	4.24	11.85	27.30	2.78	**5.23**	**54.24**
	φc	6.28	12.97	20.71	4.11	**5.09**	**50.38**

D. DC/DC AND DC/AC POWER CONVERTERS

The output PV array voltage is usually low, and in order to connect to the distribution network, this voltage must be boosted. A DC/DC boost converter can serve this purpose and maximize the electrical energy obtained from PV arrays. This boosted voltage must be therefore converted to AC voltage for connection to the network. In this article, a 5-kHz DC/DC boost converter and a 10-kHz 2L 3φ VSI are employed. To control VSI and create its switching pulses, Voltage Source Controller (VSC) strategy, as shown in Fig. 10, is applied. The VSC has two external and internal control loops. The outer loop handles the DC-link voltage and the inner one controls active and reactive components of grid currents. The modulation signals, U^*_{abc}, are created by the DC voltage controller output (I^*_d) and the outputs of the current controller (V_d, V_d) to be applied to the PWM block [28].

III. SIMULATION RESULTS

In this section, the performance evaluation of the proposed PV fed TransZSI-DVR configuration is simulated carried out, and then the results are compared to the outcomes of traditional VSI-DVR and ZSI-DVR configurations where VSI and

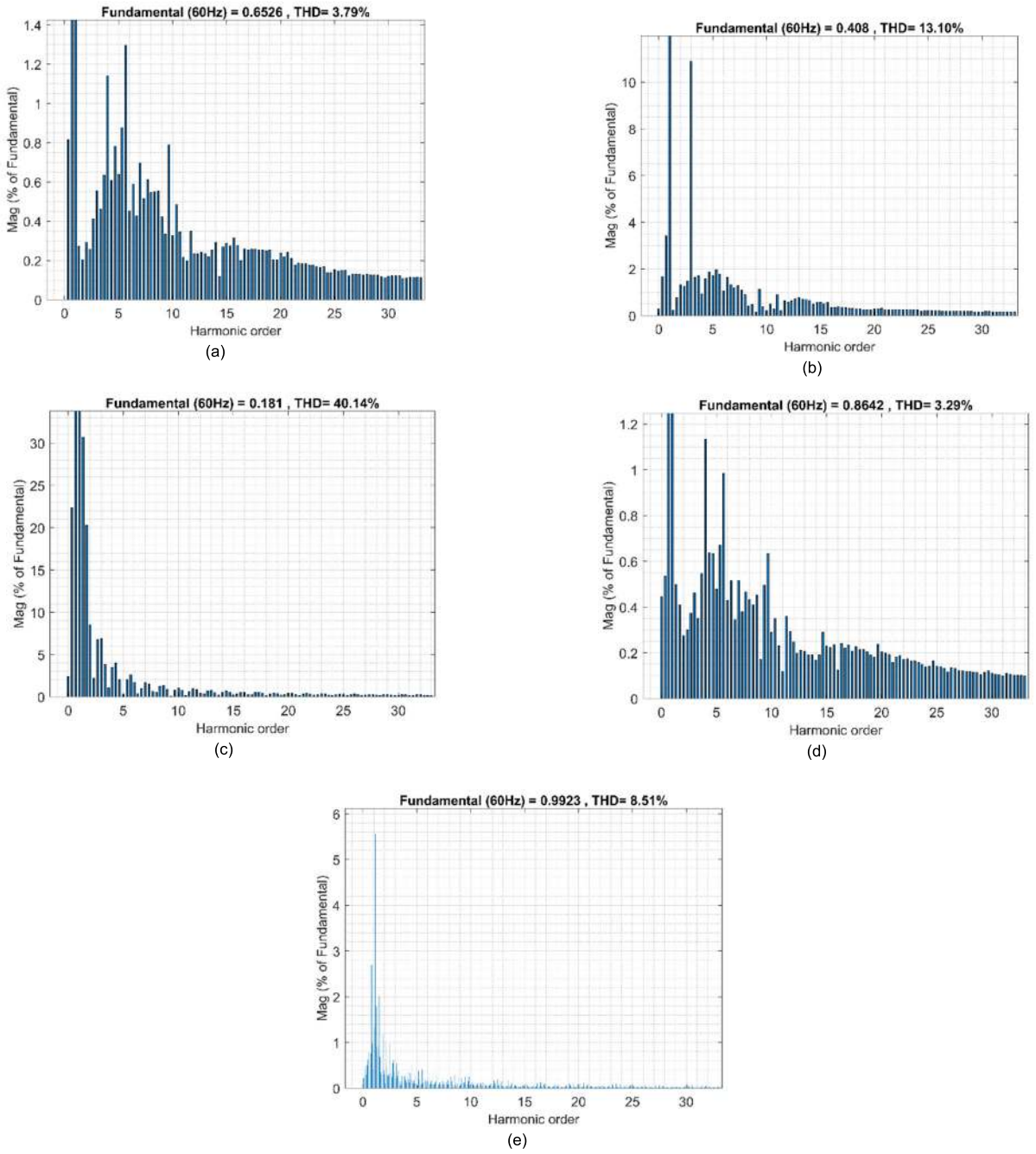

FIGURE 15. Phase A THD values of the (a) injected voltage in 0.05-0.1s, (b) injected voltage in 0.15-0.2s, (c) injected voltage in 0.25-0.3s, (d) injected voltage in 0.35-0.4s, and (e) entire load voltage in 0-0.45s.

ZSI are used, respectively. The following subsections represent three different scenarios of VSI-DVR, ZSI-DVR, and the proposed TransZSI-DVR. In all strategies presented in this article, four various voltage disturbances as severe voltage sag (75%), slight voltage sag with harmonics (50%), voltage swell (20%), and interruption (100%) are applied. The severe sag as the first voltage disturbance happens because of partial shading conditions at solar irradiation of $250W/m^2$ in the PV system. The second voltage disturbance is a slight sag with harmonics. This is also because of partial shading conditions at solar irradiation of $500W/m^2$. Swell is the third-volt disturbance which is almost caused by an abrupt reduction in load, for instance, when a large motor is turned off. The last voltage disturbance is an interruption. Faults are the common causes of interruptions. In all scenarios, the supply voltage is the PV systems' output voltage. The parameters of the grid-connected PV system and the proposed TransZSI-DVR are both given in Table 2 in the Appendix.

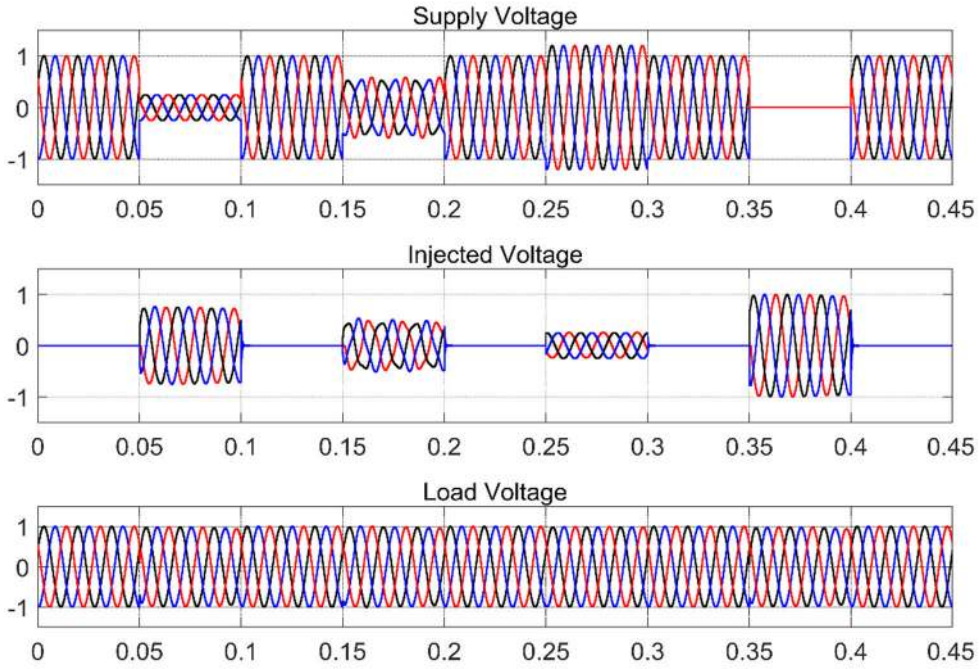

FIGURE 16. Supply, injected, and load voltage waveforms (upper, middle, and lower, respectively) in the PV fed TransZSI-DVR.

The Single Line Diagram (SLD) of the IEEE 15-bus system is shown in Fig. 11. Further information about this grid is provided in [29].

A. SCENARIO 1: VOLTAGE COMPENSATION BY VSI-DVR

In this scenario, the performance of the DVR in which a traditional VSI is used is studied. There are here two crucial matters. First, conventional VSI is a buck inverter. So, the output PV panel voltage which is usually low must be boosted. Otherwise, other power converters like cascaded multilevel VSIs that have higher voltage boost gain must deliver higher output voltage. Despite the advantages of such inverters, they have a higher cost and complex controllers. Instead, in this scenario, a boost converter before the BES is considered to increase the DC output voltage of the PV panel. Its parameters are $L = 5mH$, $C = 3000\mu F$ and $f_s = 5kHz$. Second, in this scenario, the PWM method for the modulation unit with a modulation index of 0.8 is used in VSI (see Fig. 5).

Fig. 12 depicts the supply voltage (PV systems' output voltage), the injected voltage by the VSI-DVR, and the load voltage. As seen in the middle subfigure, the magnitude of the injected voltage at the beginning of severe sag (0.05-0.1s) and interruption (0.35-0.4s) is higher than the desired voltage. This, therefore, leads to a noticeable transient in the load voltage, as shown in the lower subfigure. Also, there is a considerable delay in the desired voltage injection (middle subfigure) for voltage swell, thus, the load voltage magnitude at the beginning (0.25 0.3) is slightly changing and produces fluctuations (lower subfigure). Note that after each injected voltage interval (middle subfigure), we can observe some flickers which must be removed once there is no voltage disturbance. Figs. 13(a)-(d) present the voltage THD values (phase a) for each injected voltage of scenario 1 (VSI-DVR). The values of voltage THD for severe sag (0.05-0.1s), slight sag with harmonics (0.15-0.2s), swell (0.25-0.3s), and interruption (0.35-0.4s) are measured 10.73%, 17.79%, 45.11%, and 10.70%, respectively. Also, the full load voltage THD (phase a) is calculated at 10.12%, as shown in Fig. 13(e).

B. SCENARIO 2: VOLTAGE COMPENSATION BY ZSI-DVR

As shown earlier, VSI has some limitations. To overcome, VSI can be replaced by ZSI that has buck/boost features, higher voltage gain, lower cost, and higher efficiency. The parameters of the ZSI's X shape network, as shown in Fig. 2, are $C_1\&C_2 = 100\mu F$ and $L_1\&L_2 = 2mH$. By applying the ST duty ratio and the X shape network, the boost feature that cannot be achieved in the traditional VSI is attainable in the ZSI. This means the need for the boost converter is eliminated thereby having one power conversion and lower cost.

Fig. 14 illustrates the supply voltage (PV systems' output voltage), the injected voltage by the ZSI-DVR, and the load voltage. As shown in this figure, the problem of having a higher magnitude of the injected voltage at the beginning of severe sag and interruption is largely solved (middle subfigure). This means that the transients of the load voltage are lower (lower subfigure), as opposed to the transients of VSI-DVR. Although the delay at the beginning of the desired injected voltage with swell is reduced (middle subfigure), the fluctuations of load voltage at the beginning of 0.25-0.3s still exist (lower subfigure).

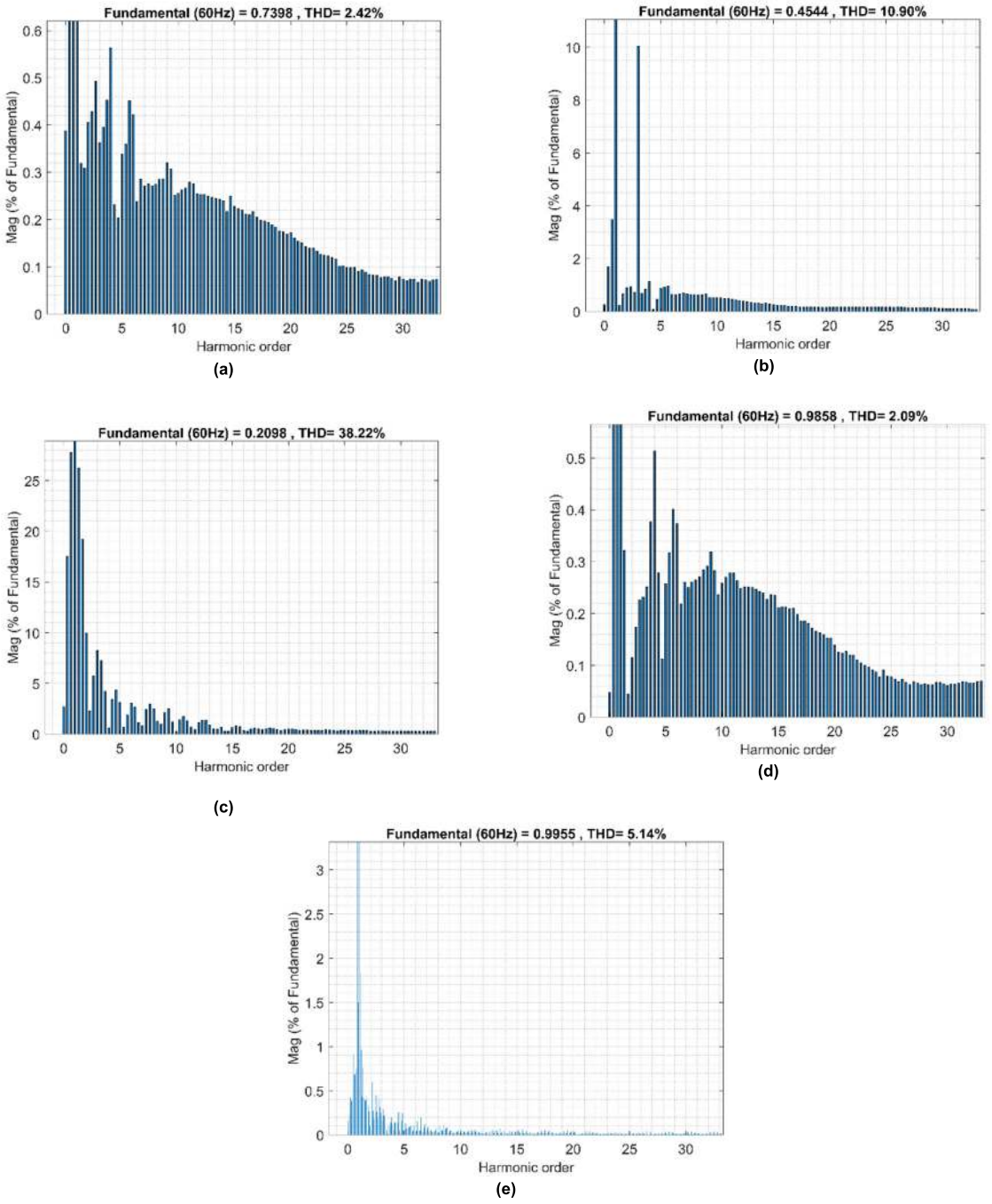

FIGURE 17. Phase A THD values of the (a) injected voltage in 0.05-0.1s, (b) injected voltage in 0.15-0.2s, (c) injected voltage in 0.25-0.3s, (d) injected voltage in 0.35-0.4s, and (e) entire load voltage in 0-0.45s.

Also, the flickers after the interval of each injected voltage are still seen (middle subfigure). Figs. 15(a)-(d) display the voltage THD values (phase a) for each injected voltage of scenario 2 (ZSI-DVR). The values of voltage THD for severe sag (0.05-0.1s), slight sag with harmonics (0.15-0.2s), swell (0.25-0.3s), and interruption (0.35-0.4s) are measured 3.79%, 13.10%, 40.14%, and 3.29%, respectively. Also, the entire load voltage THD (phase a) is calculated at 8.51%, as shown in Fig. 15(e). Compared to scenario 1 (VSI-DVR), we can infer that all the THD values in scenario 2 (ZSI-DVR) are low.

C. SCENARIO 3: VOLTAGE COMPENSATION BY TRANSZSI-DVR

Although ZSI can outperform traditional VSI, higher voltage gain without increasing the cost is of vital importance

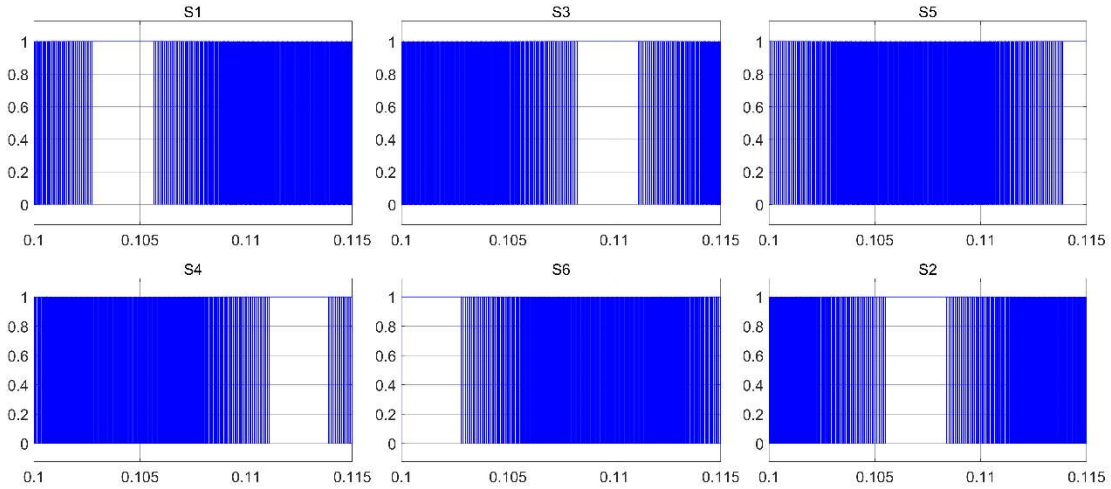

FIGURE 18. Switching pulses of TransZSI in scenario C.

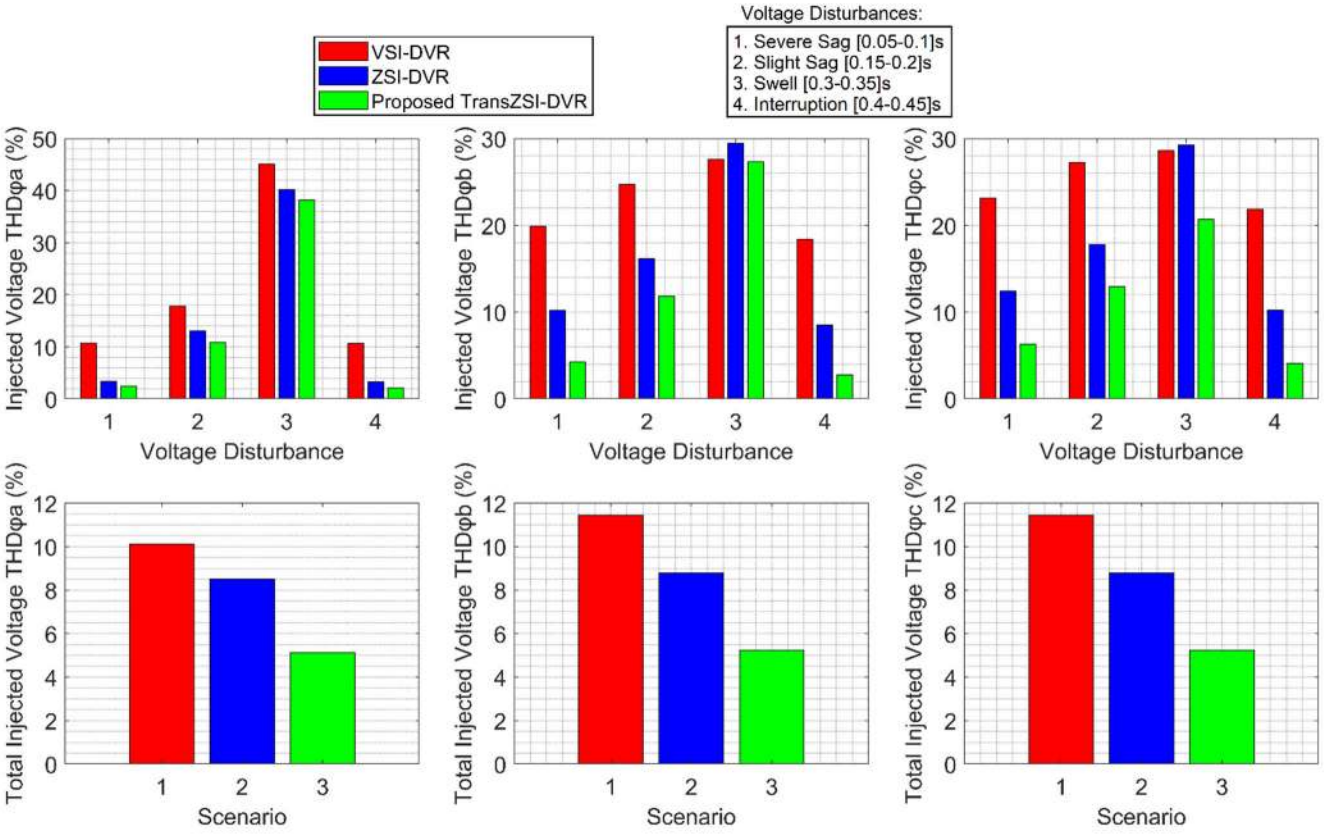

FIGURE 19. THD comparison of 3 scenarios: injected voltage THDφa (top left), injected voltage THDφb (top center), injected voltage THDφc (top right), total injected voltage THDφa (bottom left), total injected voltage THDφb (bottom center), total injected voltage THDφc (bottom right).

in the ZSI. TransZSI, as one of the ZSI's modified configurations, has a broader range of voltage conversion (by transformer's turns ratio in (10)), fewer reactive elements (Fig. 3(a)), and few element stresses (due to MCBC method). In this scenario, TransZSI with the UVT-MCBC method is proposed in the DVR configuration as the proposed TransZSI-DVR. The detailed analyses of voltage gain, voltage stress, and UVT-MCBC method have been all conducted in section 2. Fig. 16 depicts the supply voltage (PV systems' output voltage), the injected voltage by the proposed

TABLE 2. Test System Parameters.

Grid-connected PV system parameters			
Component	**Parameter**	**Value**	**Unit**
PV array SunPower SPR-305E-WHT-D	Open circuit voltage (V_{oc})	64.2	V
	Short circuit current (I_{sc})	5.96	A
	Voltage at MPP (V_{mp})	54.7	V
	Current at MPP (I_{mp})	5.58	A
	Diode saturation current (I_{sat})	$6.3014e^{-12}$	A
	Parallel R (R_p)	269.5934	Ω
	Series R (R_s)	0.037152	Ω
	Parallel strings (N_p)	66	–
	Series modules (N_s)	5	–
	PV capacitor (C_{pv1})	1000	μF
DC/DC boost converter IGBT based	Inductor (L)	5	mH
	Capacitor (C_{dc1})	6000	μF
	DC voltage (V_{dc})	273	V
	Switching frequency (f_s)	5000	Hz
DC/AC VSI IGBT based	DC voltage (V_{dc})	500	V
	Switching frequency (f_s)	1980	Hz
	Fundamental frequency	60	Hz
	Filter inductor (L_f)	10	mH
	Filter capacitor (C_f)	35	μF
Step-up transformer	Nominal apparent power (P_n)	100	kVA
	Nominal frequency (f_n)	60	Hz
	Primary voltage (V_1)	260	V
	Secondary voltage (V_2)	11	kV
Distribution grid IEEE 15-bus system	Total active power	1126.5	kW
	Total reactive power	1251.182	$kVAr$
	Nominal voltage	11	kV
TransZSI-DVR parameters			
PV panel SunPower SPR-305E-WHT-D (10*5*54.7*5.58=15.261 kW)	N_p	10	–
	N_s	5	–
	PV capacitor (C_{pv2})	1000	μF
BES Nickel-metal hydride (NiMH)	Rated capacity	200	Ah
	Nominal voltage	250	V
	Initial SOC	100	%
	Inductor (L_b)	6	mH
	Capacitor (C_b)	200	μF
DC/AC TransZSI IGBT based	DC-link capacitor (C_{dc2})	3000	μF
	Switching frequency (f_s)	10	kHz
	Capacitor (C_1)	400	μF
	Turns ratio ($n_2:n_1$)	2:1	–
	Modulation index (M)	0.93	–
	ST duty ratio (D_{sh})	0.2	–
	Filter capacitor (C_f)	40	μF
	Filter inductor (L_f)	1	mH
Three series transformers	Nominal apparent power (P_n)	25	kVA
	Nominal frequency (f_n)	60	Hz
	Primary voltage (V_1)	130	V
	Secondary voltage (V_2)	11	kV

TransZSI-DVR, and the load voltage. Based on this figure, all the voltage disturbances are thoroughly compensated for. The issue related to the higher magnitude of the injected voltage at the beginning of severe sag and interruption is wholly addressed which confirms the accurate detection of the UVT controller in the UVT-MCBC method. Also, the transients of the load voltage are the lowest, as opposed to the transients of VSI-DVR and ZSI-DVR. With swell, the delay at the beginning of the desired voltage is minimized more than before, the fluctuations of load voltage at the beginning (0.25-0.3s) do not exist anymore. This is because of the MCBC controller which reduces the transients to the lowest possible value. The flickers after the interval of each injected voltage are removed, which means the UVT-MCBC accurately and successfully detects the start and stop points of all voltage disturbances. The proposed TransZSI-DVR can produce the best load voltage. This is of the utmost importance for sensitive and critical loads. Figs. 17(a)-(d) show the voltage THD values (phase a) for each injected voltage of scenario 3 in which TransZSI-DVR is proposed. The values of voltage THD for severe sag (0.05-0.1s), slight sag with harmonics (0.15-0.2s), swell (0.25-0.3s), and interruption (0.35-0.4s) are measured 2.42%, 10.90%, 38.22%, and 2.09%, respectively. Also, the full load voltage THD (phase a) is calculated at 5.14%, as shown in Fig. 17(e). Compared to scenario 1 (VSI-DVR) and scenario 2 (ZSI-DVR), we can conclude that all the THD values in scenario 3 with the proposed TransZSI-DVR are the lowest. As shown before in (17), by keeping the ST duty ratio unchanged, the lowest harmonics among the other two traditional DVRs can be achieved. Also, the switching pulses of TransZSI in this scenario are shown in Fig. 18. The tabular and graphical comparisons of voltage THD values (phase a, b, and c, and total period) measured in each DVR scenario are provided by Table 1 and Fig. 19, respectively.

IV. CONCLUSION

In this work, a new PV fed TransZSI-DVR has been presented to enhance the power quality of PV systems. Compared to traditional VSI-DVR and ZSI configurations, the proposed Trans-ZSIDVR brings significant benefits like being a buck and boost converter simultaneously, fewer passive components, broader voltage gain, and lower voltage stress on switches. For accurate detection and adequate compensation for voltage disturbances, the UVT-MCBC method has been implemented for TransZSI-DVR. Four different voltage disturbances such as severe sag (75%), slight sag with harmonics (50%), swell (20%), and interruption (100%) have been considered for performance evaluation of the proposed TransZSI-DVR with UVT-MCBC. Such voltage disturbances have been tested in three different DVR scenarios. The theoretical analysis and simulation results have significantly substantiated the performance of the proposed TransZSI-DVR in terms of sufficient compensation for sag/swell/interruption,

a considerable reduction in voltage THD harmonics, power quality enhancement of injected voltage to the PCC and PV system's output voltage as well.

The scopes for future research will be many some of which could be as follows. Research into modified DVR control methods to improve the power quality of injected voltage to the PCC in terms of its magnitude, harmonics, and also accurate detection of start/stop point of the voltage disturbance better than before. Another research spot would be the configuration of the inverter used in the DVR to reduce the cost, weight, and volume of the inverter, thereby decreasing the overall DVR cost. Last but not least, the stability of the proposed DVR system can be also studied, especially for remote areas where the stability of power is important.

APPENDIX

See Table 2.

REFERENCES

[1] R. Teodorescu, M. Liserre, and P. Rodriguez, *Grid Converters for Photovoltaic and Wind Power Systems*. Piscataway, NJ, USA: Wiley, 2011.
[2] G. S. Chawda, A. G. Shaik, M. Shaik, S. Padmanaban, J. B. Holm-Nielsen, O. P. Mahela, and P. Kaliannan, "Comprehensive review on detection and classification of power quality disturbances in utility grid with renewable energy penetration," *IEEE Access*, vol. 8, pp. 146807–146830, 2020.
[3] A. A. Sallam and O. P. Malik, "Electric power quality," in *Electric distribution Systems*. Piscataway, NJ, USA: Wiley, 2019, pp. 295–319.
[4] G. S. Chawda, A. G. Shaik, O. P. Mahela, S. Padmanaban, and J. B. Holm-Nielsen, "Comprehensive review of distributed FACTS control algorithms for power quality enhancement in utility grid with renewable energy penetration," *IEEE Access*, vol. 8, pp. 107614–107634, 2020.
[5] Y. Han, Y. Feng, P. Yang, L. Xu, Y. Xu, and F. Blaabjerg, "Cause, classification of voltage sag, and voltage sag emulators and applications: A comprehensive overview," *IEEE Access*, vol. 8, pp. 1922–1934, 2020.
[6] *IEEE Recommended Practice for Monitoring Electric Power Quality*, IEEE Standard 1159-1995, 1995.
[7] A. Ghosh and G. Ledwich, "Custom power devices: An introduction," in *Power Quality Enhancement Using Custom Power Devices*. Boston, MA, USA: Springer, 2002, pp. 113–136.
[8] A. Moghassemi and S. Padmanaban, "Dynamic voltage restorer (DVR): A comprehensive review of topologies, power converters, control methods, and modified configurations," *Energies*, vol. 13, no. 16, p. 4152, Aug. 2020.
[9] M. Prasad and A. K. Akella, "Voltage and current quality improvement by solar photovoltaic fed ZSI-DVR," *Procedia Comput. Sci.*, vol. 125, pp. 434–441, 2018.
[10] J. Olamaei, S. Ebrahimi, and A. Moghassemi, "Compensation of voltage sag caused by partial shading in grid-connected PV system through the three-level SVM inverter," *Sustain. Energy Technol. Assessments*, vol. 18, pp. 107–118, Dec. 2016.
[11] A. Abdelhakim, F. Blaabjerg, and P. Mattavelli, "Modulation schemes of the three-phase impedance source inverters—Part I: Classification and review," *IEEE Trans. Ind. Electron.*, vol. 65, no. 8, pp. 6309–6320, Aug. 2018.
[12] D. Vilathgamuwa, C. Gajanayake, P. Loh, and Y. Li, "Voltage sag compensation with Z-Source inverter based dynamic voltage restorer," in *Proc. Conf. Rec. IEEE Ind. Appl. Conf. 41st IAS Annu. Meeting*, Tampa, FL, USA, Oct. 2006, pp. 2242–2248.
[13] M. Rajkumar and S. R. Reddy, "Modeling and simulation of ZSI based DVR for voltage compensation," in *Proc. Int. Conf. Comput., Commun. Electr. Technol. (ICCCET)*, Tamil Nadu, India, Mar. 2011, pp. 346–351.
[14] M. D. Fayaz and B. Veeranna, "Voltage sag/swell compensation using Z-source inverter DVR based on fuzzy controller," *Int. J. Adv. Technol. Innov. Res.*, vol. 7, no. 8, pp. 1262–1268, 2015.
[15] C. Gopinath and R. Ramesh, "Design and implementation of Z-source inverter based DVR," *Eur. J. Sci. Res.*, vol. 57, no. 3, pp. 514–523, 2011.
[16] J. Ajay Daniel, C. Gopinath, and R. Ramesh, "Z source inverter based dynamic voltage restorer using super capacitor to mitigate voltage SAG and voltage swell," in *Proc. Int. Conf. Circuits, Power Comput. Technol. (ICCPCT)*, Nagercoil, India, Mar. 2013, pp. 37–42.
[17] O. Ellabban and H. Abu-Rub, "Z-source inverter: Topology improvements review," *IEEE Ind. Electron. Mag.*, vol. 10, no. 1, pp. 6–24, Mar. 2016.
[18] M. R. Banaei and A. R. Dehghanzadeh, "A novel Z-source based multilevel inverter for renewable sources fed DVR," in *Proc. 1st Power Qual. Conf.*, Tehran, Iran, 2010, pp. 1–6.
[19] C. V. Deshpande and S. A. Deokar, "Enhancement of power quality using dynamic voltage restorer based on EZ source inverter," *Int. J. Adv. Res. Electr., Electron. Instrum. Eng.*, vol. 4, no. 2, pp. 1004–1013, 2015.
[20] N. N. Gopal and M. S. Abirami, "A dynamic voltage restorer system by modified Z-source inverter to mitigate voltage sag," *Int. J. Appl. Eng. Res.*, vol. 13, no. 10, pp. 7970–7976, 2018.
[21] J. Chakravorty and G. Sharma, "DVR with modified y source inverter and MCFC," *Eng., Technol. Appl. Sci. Res.*, vol. 9, no. 1, pp. 3803–3806, Feb. 2019.
[22] H. Prajapati, M. Vekaria, N. Joshi, M. Parikh, and H. Solanki, "Compensation of voltage sag and swell by unit vector template generation technique and synchronous reference frame theory for dynamic voltage restorer," *Int. J. Sci. Res. Develop.*, vol. 6, no. 1, pp. 0613–2321, 2018.
[23] M. Shen, J. Wang, A. Joseph, F. Zheng Peng, L. M. Tolbert, and D. J. Adams, "Constant boost control of the Z-source inverter to minimize current ripple and voltage stress," *IEEE Trans. Ind. Appl.*, vol. 42, no. 3, pp. 770–778, May 2006.
[24] Y. Liu, B. Ge, H. Abu-Rub, and F. Blaabjerg, "Single-phase Z-sourcequasi-Z-source inverters and converters: An overview of double-line-frequency power-decoupling methods and perspectives," *IEEE Ind. Electron. Mag.*, vol. 12, no. 2, pp. 6–23, Jun. 2018.
[25] R. Haste, A. Matre, and S. L. Shaikh, "Power quality improvement in grid connected renewable energy sources at distribution level," in *Proc. Int. Conf. Circuits, Power Comput. Technol. [ICCPCT-]*, Nagercoil, India, Mar. 2014, pp. 496–502.
[26] A. Abdelhakim, F. Blaabjerg, and P. Mattavelli, "Modulation schemes of the three-phase impedance source inverters—Part II: Comparative assessment," *IEEE Trans. Ind. Electron.*, vol. 65, no. 8, pp. 6321–6332, Aug. 2018.
[27] A. Moghassemi, S. Ebrahimi, and J. Olamaei, "Maximum power point tracking methods used in photovoltaic systems: A review," *Signal Process. Renew. Energy*, vol. 4, no. 3, pp. 19–39, 2020.
[28] J. Kasera, V. Kumar, R. R. Joshi, and J. K. Maherchandani, "Design of grid connected photovoltaic system employing incremental conductance MPPT algorithm," *J. Electr. Eng.*, vol. 12, pp. 172–177, 2012.
[29] M. Singh, B. K. Panigrahi, A. R. Abhyankar, R. Mukherjee, and R. Kundu, "Optimal location, size and protection coordination of distributed generation in distribution network," in *Proc. IEEE Symp. Swarm Intell. (SIS)*, Singapore, Apr. 2013, pp. 221–227.

ALI MOGHASSEMI received the B.Sc. and M.Sc. degrees in electrical power engineering from Islamic Azad University, South Tehran Branch, Tehran, Iran, in 2012 and 2015, respectively. He is currently a University Lecturer with the University of Applied Sciences and Technology, Tehran, and also an External Researcher with the Department of Energy Technology, Aalborg University, Esbjerg, Denmark. He has authored or coauthored more than 15 scientific articles in international journals and conferences. He has also published a book and coauthored two book chapters. His current research interests include renewable energy technologies, partial shaded PV, MPPT algorithm, power quality, DVR, voltage disturbances, harmonic, power electronics, Z-source inverter, and Switching Control strategy. Since June 2018, he has been serving as a reviewer for several high-quality journals.

SANJEEVIKUMAR PADMANABAN (Senior Member, IEEE) received the bachelor's degree in electrical engineering from the University of Madras, Chennai, India, in 2002, the master's degree (Hons.) in electrical engineering from Pondicherry University, Pondicherry, India, in 2006, and the Ph.D. degree in electrical engineering from the University of Bologna, Bologna, Italy, in 2012. From 2012 to 2013, he was an Associate Professor with VIT University. In 2013, he joined the National Institute of Technology, India, as a Faculty Member. In 2014, he was invited as a Visiting Researcher with the Department of Electrical Engineering, Qatar University, Doha, Qatar, funded by the Qatar National Research Foundation (Government of Qatar). He continued his research activities with the Dublin Institute of Technology, Dublin, Ireland, in 2014. From 2016 to 2018, he has served as an Associate Professor for the Department of Electrical and Electronics Engineering, University of Johannesburg, Johannesburg, South Africa. Since 2018, he has been a Faculty Member with the Department of Energy Technology, Aalborg University, Esbjerg, Denmark. He has authored more than 300 scientific articles. He is also a Fellow of the Institution of Engineers, India, of the Institution of Electronics and Telecommunication Engineers, India, and of the Institution of Engineering and Technology, U.K. He was a recipient of the Best Paper cum Most Excellence Research Paper Award from IET-SEISCON'13, IET-CEAT'16, IEEE-EECSI'19, and IEEE-CENCON'19, and five best paper awards from ETAEERE'16 sponsored Lecture Notes in electrical engineering, Springer book. He is also an editor/associate editor/editorial board of refereed journals, in particular, the IEEE Systems Journal, the IEEE Transaction on Industry Applications, IEEE Access, *IET Power Electronics*, *IET Electronics Letters*, and *International Transactions on Electrical Energy Systems* (Wiley), a Subject Editorial Board Member of *Energy Sources*, *Energies Journal*, and MDPI, and the Subject Editor of the *IET Renewable Power Generation*, *IET Generation, Transmission and Distribution*, and *Obesity Facts* journal (Canada).

VIGNA K. RAMACHANDARAMURTHY (Senior Member, IEEE) received the bachelor's degree (Hons.) in electrical and electronics engineering and the Ph.D. degree from the University of Manchester Institute of Science and Technology (UMIST), U.K., in 1998 and 2001, respectively. He is currently a Professor with the Institute of Power Engineering, Universiti Tenaga Nasional, Malaysia. He is also a Chartered Engineer registered with the Engineering Council of U.K., and a Professional Engineer registered with the Board of Engineers, Malaysia. He strongly advocates industrial based research. He is also a Consultant for Malaysia's electrical utility and has completed more than 300 projects in renewable energy and smart grid. He led and developed several technical guidelines for distributed generation, solar PV, electric vehicle, and energy storage for Malaysia. His current research interests include power systems related studies, renewable energy, energy storage, smart grid, power quality, electric vehicle, and rural electrification. He has served as an electrical engineer in Malaysia and has experience working in the distribution and transmission systems, and power plant. He has received many awards for research and leadership. In 2008, he received the IET Mike Sargeant Award. In 2009, he received the prestigious Institution of Engineers Malaysia (IEM) Young Engineers Award. He was also the recipient of the Best Researcher Award for several years and has won several gold medals at the International Invention Competition. He is also an Associate Editor of *IET Smart Grid*, IET RPG, IEEE Smart Grid, and IEEE Access.

MASSIMO MITOLO (Fellow, IEEE) received the Ph.D. degree in electrical engineering from the University of Napoli Federico II, Italy, in 1990. He is currently a Full Professor of electrical engineering with the Irvine Valley College, Irvine, CA, USA, and also a Senior Consultant in electric power engineering with Engineering Systems, Inc., ESi. He has authored more than 118 journal articles and the books *Electrical Safety of Low-Voltage Systems* (McGraw-Hill, 2009) and *Laboratory Manual for Introduction to Electronics: A Basic Approach* (Pearson, 2013). His research interests include the analysis and grounding of power systems and electrical safety engineering.

Dr. Mitolo was a recipient of many recognitions and best paper awards, including the IEEE-I&CPS Ralph H. Lee Department Prize Paper Award, the IEEE-I&CPS 2015 Department Achievement Award, and the IEEE Region 6 Outstanding Engineer Award. He is currently the Deputy Editor-in-Chief of the IEEE Transactions on Industry Applications. He is active within the Industrial and Commercial Power Systems Department of the IEEE Industry Applications Society (IAS) in many committees and working groups. He also serves as an Associate Editor for the IEEE IAS Transactions. He is a registered Professional Engineer in the state of California and Italy.

MOHAMED BENBOUZID (Fellow, IEEE) received the B.Sc. degree in electrical engineering from the University of Batna, Batna, Algeria, in 1990, the M.Sc. and Ph.D. degrees in electrical and computer engineering from the National Polytechnic Institute of Grenoble, Grenoble, France, in 1991 and 1994, respectively, and the Habilitation à Diriger des Recherches degree from the University of Picardie "Jules Verne," Amiens, France, in 2000. After receiving the Ph.D. degree, he joined the Professional Institute of Amiens, the University of Picardie "Jules Verne," where he was an Associate Professor of electrical and computer engineering. Since September 2004, he has been with the University of Brest, Brest, France, where he is currently a Full Professor of electrical engineering. He is currently a Distinguished Professor and also a 1000 Talent Expert with Shanghai Maritime University, Shanghai, China. His current research interests include the analysis, design, and control of electric machines, variable-speed drives for traction, propulsion, and renewable energy applications, and fault diagnosis of electric machines.

Dr. Benbouzid has been elevated as an IEEE Fellow for his contributions to diagnosis and fault-tolerant control of electric machines and drives. He is also a Fellow of the IET. He is the Editor-in-Chief of the *International Journal on Energy Conversion* and the *Applied Sciences* (MDPI) Section on Electrical, Electronics and Communications Engineering. He is a Subject Editor for *IETRenewable Power Generation*. He is also an Associate Editor of the IEEE Transactions on Energy Conversion.